-5873C

Sandia National Laboratories

Uncertainty Quantification in Computational Modeling of Plasma-Surface Interactions

Pieterjan Robbe, Tiernan Casey, Khachik Sargsyan, Habib Najm

May 5, 2022

Sandia National Laboratories is a multimission laboratory managed and operated by National Technology and Engineering Solutions of Sandia, LLC, a wholly owned subsidiary of Honeywell International, Inc.,

dia National Laboratories is a multimission laboratory managed and operated by National Technology & Engineering Solutions of Sandia, LLC, a wholly ow subsidiary of Honeywell International Inc., for the U.S. Department of Energy's National Nuclear Security Administration under contract DE-NA0003525.

Plasma-surface interactions

- Modeling and simulation of the interaction between the boundary plasma and the material surface in a fusion device
- Challenges are addressed in the PSI2 SciDAC project [Wirth et al., 2022]
  - SOLPS computation of plasma background conditions
  - hPIC sheath plasma computation and Ion Energy-Angle Distribution (IEAD)
  - GITR macroscopic global impurity transport computations
  - F-Tridyn ion-solid interaction particle-based simulations
  - Xolotl material surface evolution

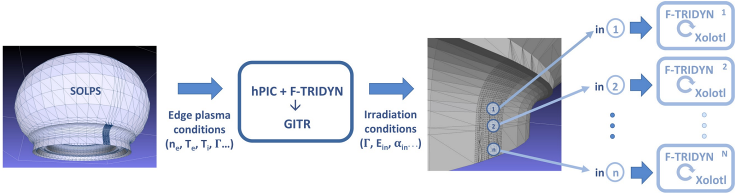

- Code coupling within the Integrated Plasma Simulation (IPS) framework [Elwasif et al., 2010]

Plasma-surface interaction atomistic model

- Tungsten (●) lattice irradiated by helium atoms (●)

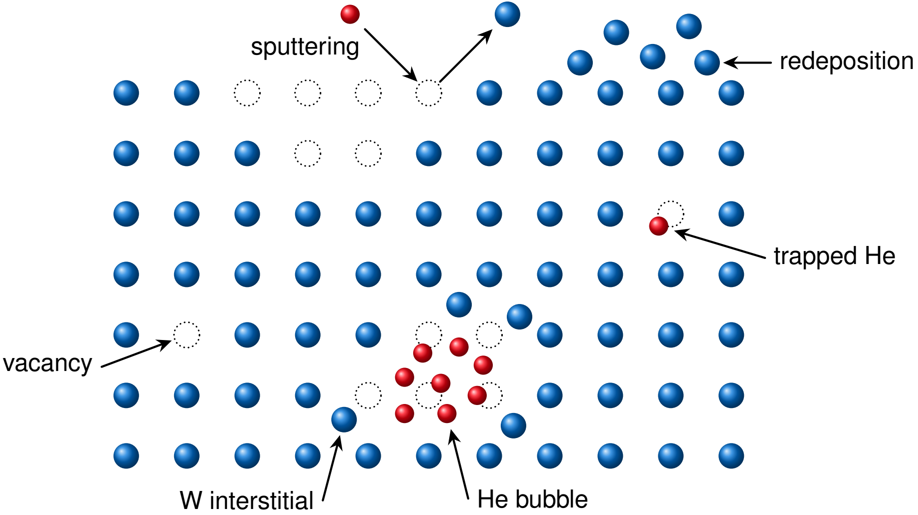

Simulation of plasma-surface interactions

- Multi-physics coupled code simulates material evolution in plasma-surface interactions
  - F-Tridyn: Monte Carlo Binary Collision Approximation particle code for simulating ion interactions with rough surfaces [Drobny et al., 2017]
  - Xolotl: spatially-dependent cluster dynamics code for simulating the PDEs that describe the evolution of tungsten under irradiation [Blondel et al., 2017]

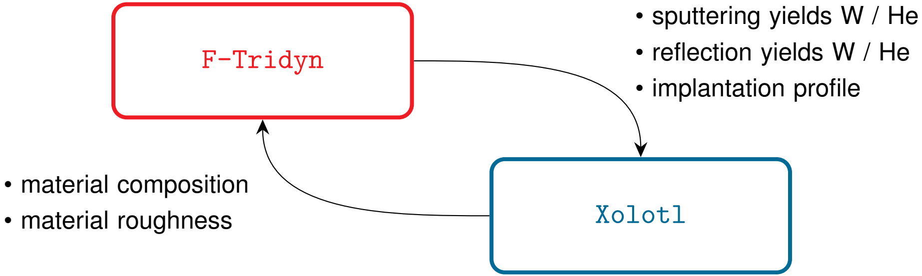

F-Tridyn–Xolotl interaction

F-Tridyn

- Simulate ion-solid interactions by tracking the trajectories of energetic helium ions through a tungsten target
- Monte Carlo approach simulates individual particles (~ 100,000)
- Quantities of interest are sputtering and reflection coefficients and implantation profile

Xolotl

- Tungsten material represented by the concentration of He clusters at each spatial grid point
- Reaction-diffusion equation for the evolution of the cluster concentrations

$$\frac{\mathrm{d}C}{\mathrm{d}t} = \underbrace{\phi \cdot \rho}_{\text{incoming He flux}} \underbrace{-\nabla^2(-D\nabla C + uC)}_{\text{diffusion \& drift}} \underbrace{-Q(C)}_{\text{reaction term}}$$

solved using finite difference approach in PETSc [Balay et al., 2022], parallelized using MPI

- Quantities of interest are He retention and surface growth as a function of time
- Surface evolution influenced by trap mutation (+), sputtering (–) and redeposition (+)

Polynomial chaos expansions

- A polynomial chaos expansion (PCE) surrogate model for the system response $P(\boldsymbol{x})$ can be written as

$$\mathcal{P}(\boldsymbol{x}) := \sum_{\boldsymbol{u}\in\mathcal{I}} c_{\boldsymbol{u}}\psi_{\boldsymbol{u}}(\boldsymbol{\xi})$$

  where $c_{\boldsymbol{u}}$ is a coefficient, $\psi_{\boldsymbol{u}}$ is a multivariate orthogonal polynomial in terms of the random variables $\boldsymbol{\xi} = (\xi_1, \xi_2, \ldots, \xi_d) \in X \subseteq \mathbb{R}_0^d$, and $\boldsymbol{u} \in \mathbb{N}_0^d$ is a multi-index [Xiu and Karniadakis, 2002] [Ghanem and Spanos, 2003]
- Usually, the basis functions $\psi_{\boldsymbol{u}}(\boldsymbol{\xi})$ are orthonormal with respect to a weight function $w(\boldsymbol{\xi})$, i.e.,

$$\int_X w(\boldsymbol{\xi})\psi_{\boldsymbol{u}_r}(\boldsymbol{\xi})\psi_{\boldsymbol{u}_s}(\boldsymbol{\xi})\mathrm{d}\boldsymbol{\xi} = \delta_{r,s}$$

  where $\delta_{r,s}$ is the Kronecker delta and $\boldsymbol{u}_r$ and $\boldsymbol{u}_s$ are two multi-indices
- When the random variables $\boldsymbol{\xi}$ are i.i.d., we can express the basis functions as

$$\psi_{\boldsymbol{u}}(\boldsymbol{\xi}) = \prod_{j=1}^{d} \psi_{\boldsymbol{u}_j}(\xi_j)$$

Bayesian compressive sensing

- Given ranges $[a_j, b_j]$ for the parameters x_j, $j = 1, 2, \ldots, d$, we assume the linear relation

$$x_j = \frac{a_j + b_j}{2} + \frac{b_j - a_j}{2}\xi_j$$

and the $\psi_{\boldsymbol{u}}(\boldsymbol{\xi})$ are multivariate Legendre polynomials

- Given a set of input-output measurements $\{(\boldsymbol{x}_n, P(\boldsymbol{x}_n))\}_{n=1}^{N}$, the coefficients of the PCE can be found using, e.g., least-squares regression
- For a high number of dimensions d and a reasonably high polynomial order, the problem of obtaining the coefficients $\boldsymbol{c} = \{c_{\boldsymbol{u}}\}_{\boldsymbol{u}\in\mathcal{I}}$ is underdetermined
- In Bayesian compressive sensing (BCS), we solve the regularized optimization problem [Sargsyan et al., 2014]

$$\operatorname*{argmax}_{\boldsymbol{c}}\{\log \mathcal{L}_D(\boldsymbol{c}) - \alpha\|\boldsymbol{c}\|_1\}$$

- To further avoid overfitting, we use an iterative approach that gradually increases the index set size and take the common basis terms from a number of different tries

Global sensitivity analysis with polynomial chaos expansions

- The mean and variance of the PCE can be computed directly from the coefficients

$$\mathbb{E}\left[\mathcal{P}(\boldsymbol{x})\right] = c_{\boldsymbol{0}} \quad \text{and} \quad \mathbb{V}\left[\mathcal{P}(\boldsymbol{x})\right] = \sum_{\substack{\boldsymbol{u}\in\mathcal{I} \\ \boldsymbol{u}\neq\boldsymbol{0}}} c_{\boldsymbol{u}}^2$$

- In variance-based sensitivity analysis, we compute Sobol' indices that express what amount of the total output variance can be attributed to which (set of) parameters [Sobol, 2001]
- The total-effect Sobol' sensitivity indices can be extracted as

$$S_j^{\text{total}} = \left(\mathbb{V}\left[\mathcal{P}(\boldsymbol{x})\right]\right)^{-1} \cdot \sum_{\boldsymbol{u}\in\mathcal{J}_j} c_{\boldsymbol{u}}^2$$

where $\mathcal{J}_j = \left\{\boldsymbol{u} \in \mathcal{I} \middle| u_j > 0\right\}$ for $j = 1, 2, \ldots, d$ [Sudret, 2008] [Crestaux et al., 2009]

Multifidelity polynomial chaos expansion (1/2)

- Assume we have two models that predict the system response at two different fidelity levels $P^{\text{high}}(\boldsymbol{x})$ and $P^{\text{low}}(\boldsymbol{x})$, then trivially

$$P^{\text{high}}(\boldsymbol{x}) = P^{\text{low}}(\boldsymbol{x}) + (P^{\text{high}}(\boldsymbol{x}) - P^{\text{low}}(\boldsymbol{x})) = P^{\text{low}}(\boldsymbol{x}) + P^{\text{corr}}(\boldsymbol{x})$$

- Constructing a PCE for both terms in the right-hand side, we obtain the multifidelity polynomial chaos expansion (MF-PCE) [Ng and Eldred, 2012]

$$\mathcal{P}^{\text{mf}}(\boldsymbol{x}) := \sum_{\boldsymbol{u} \in \mathcal{I}^{\text{low}}} c_{\boldsymbol{u}}^{\text{low}} \psi_{\boldsymbol{u}}(\boldsymbol{\xi}) + \sum_{\boldsymbol{u} \in \mathcal{I}^{\text{corr}}} c_{\boldsymbol{u}}^{\text{corr}} \psi_{\boldsymbol{u}}(\boldsymbol{\xi})$$

  where $c_{\boldsymbol{u}}^{\text{low}}$ and $\mathcal{I}^{\text{low}}$, and $c_{\boldsymbol{u}}^{\text{corr}}$ and $\mathcal{I}^{\text{corr}}$ are the coefficients and index sets of the low-fidelity and the correction term respectively

- We require $\mathcal{I}^{\text{corr}} \subseteq \mathcal{I}^{\text{low}}$ so that (ideally) we require less expensive model evaluations to compose the correction term PCE compared to the number of cheap model evaluations required to compose the low-fidelity PCE

Multifidelity polynomial chaos expansion (2/2)

- The MF-PCE can be rewritten as

$$\mathcal{P}^{\text{mf}}(\boldsymbol{x}) = \sum_{\boldsymbol{u}\in\mathcal{I}^{\text{corr}}} (c_{\boldsymbol{u}}^{\text{low}} + c_{\boldsymbol{u}}^{\text{corr}})\psi_{\boldsymbol{u}}(\boldsymbol{\xi}) + \sum_{\boldsymbol{u}\in\mathcal{I}^{\text{low}}\setminus\mathcal{I}^{\text{corr}}} c_{\boldsymbol{u}}^{\text{low}}\psi_{\boldsymbol{u}}(\boldsymbol{\xi})$$

  so that Sobol' sensitivity indices can be extracted in the usual way
- The MF-PCE construction is more efficient if
  1. The correction term is less complex than the high-fidelity model, resulting in a faster decay of the PCE coefficients
  2. The initial stochastic error (variance) for the correction term is lower, which is the result if the low- and high-fidelity model are strongly correlated
- The variance of the correction term is

$$\begin{aligned}\mathbb{V}\left[P^{\text{corr}}(\boldsymbol{x})\right] &= \mathbb{V}\left[P^{\text{high}}(\boldsymbol{x}) - P^{\text{low}}(\boldsymbol{x})\right] \\ &= \mathbb{V}\left[P^{\text{high}}(\boldsymbol{x})\right] + \mathbb{V}\left[P^{\text{low}}(\boldsymbol{x})\right] - 2\,\text{cov}(P^{\text{high}}(\boldsymbol{x}), P^{\text{low}}(\boldsymbol{x}))\end{aligned}$$

Numerical experiments setup

- PISCES-A linear plasma device used to study scenarios relevant to divertor design in fusion devices
- 1D geometry with 256 grid cells, 1s of exposure, perform F-Tridyn and Xolotl in turn within each time step

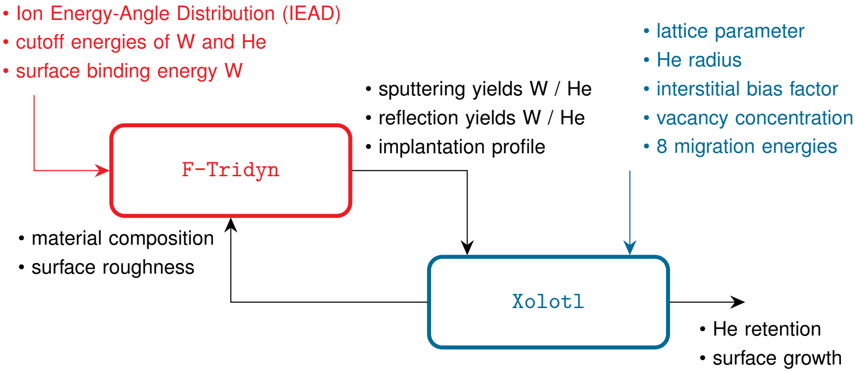

PCE surrogate construction for F-Tridyn

- Construct surrogate model for `F-Tridyn` prediction of sputtering yield of tungsten
- PCE coefficients obtained using iterative BCS with 1000 training samples and 100 validation samples, ~25 minutes per sample on 2 nodes (136 cores) on Cori
- Comparison of actual model output and PCE prediction shows good agreement

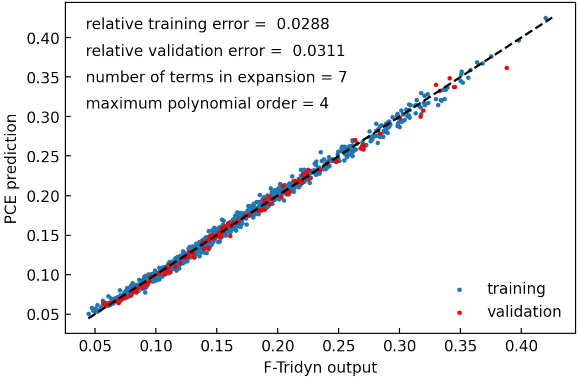

Global sensitivity analysis of F-Tridyn

- Convergence of the total-effect Sobol' sensitivity indices as a function of the number of training samples
- Values of the sensitivity indices stabilize after ~100 samples

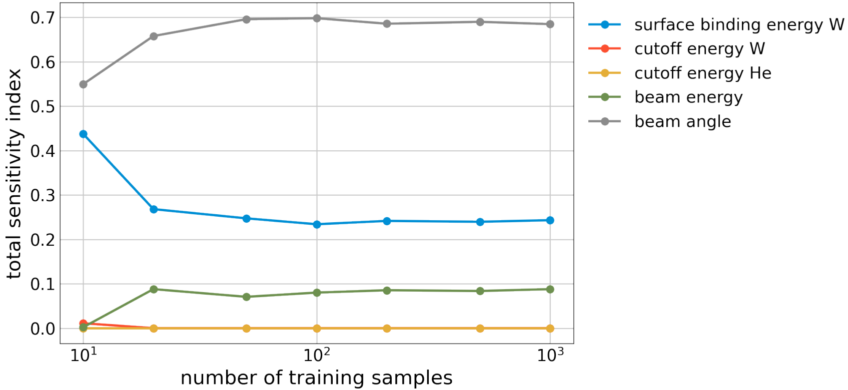

Multifidelity setup for F-Tridyn

- Samples of the high-fidelity model $P^{\text{high}}(\boldsymbol{x})$ use 100,000 particles
- Consider a low-fidelty model $P^{\text{low}}(\boldsymbol{x})$ that uses only 10,000 particles, ~5 minutes per sample
- Correlogram between high-fidelity and low-fidelity model output shows good correlation

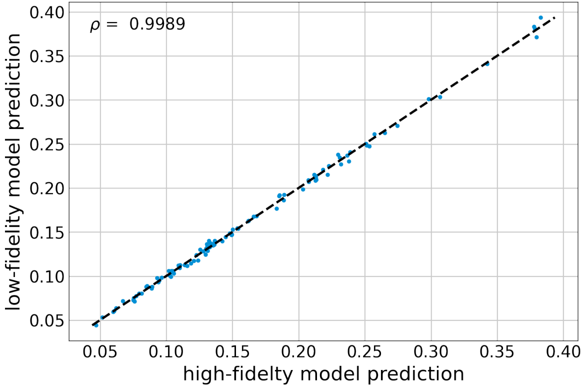

Multifidelity global sensitivity analysis of F-Tridyn (1/2)

- Use the multifidelity PCE implementation in Dakota [Adams et al., 2021]
- Values of the sensitivity indices stabilize after the equivalent of ~30 high-fidelity samples

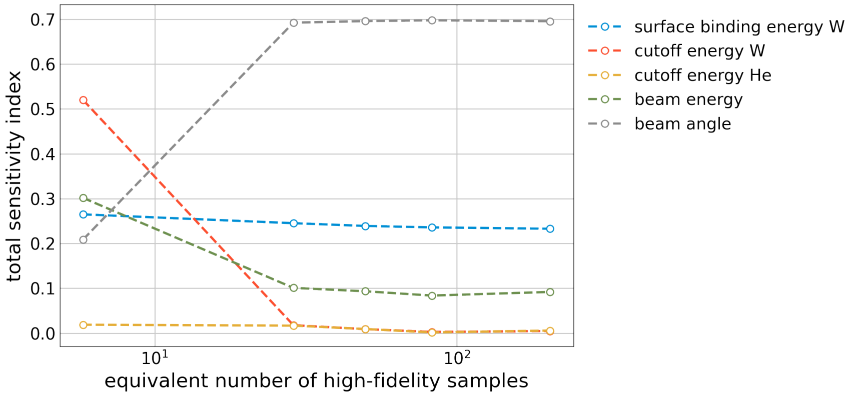

Multifidelity global sensitivity analysis of F-Tridyn (2/2)

- Use the multifidelity PCE implementation in Dakota [Adams et al., 2021]
- Values of the sensitivity indices stabilize after the equivalent of ~30 high-fidelity samples

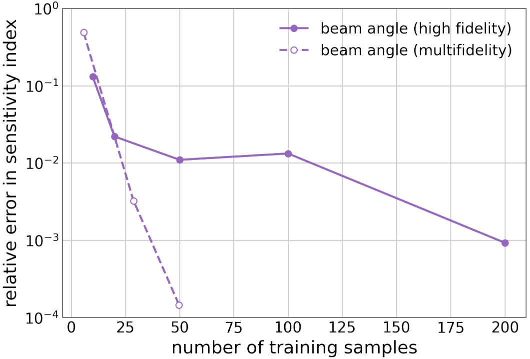

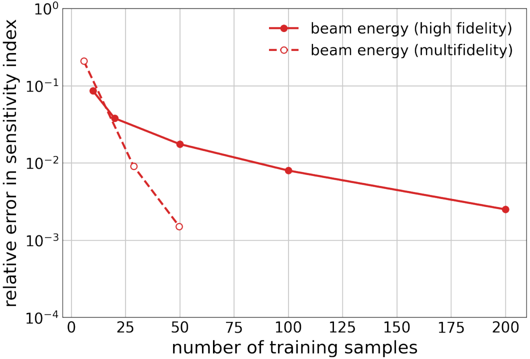

Coupled Xolotl-FTridyn (1/2)

- Output quantities of interest are surface growth and He retention as a function of time
- Illustration of 25 randomly chosen output samples

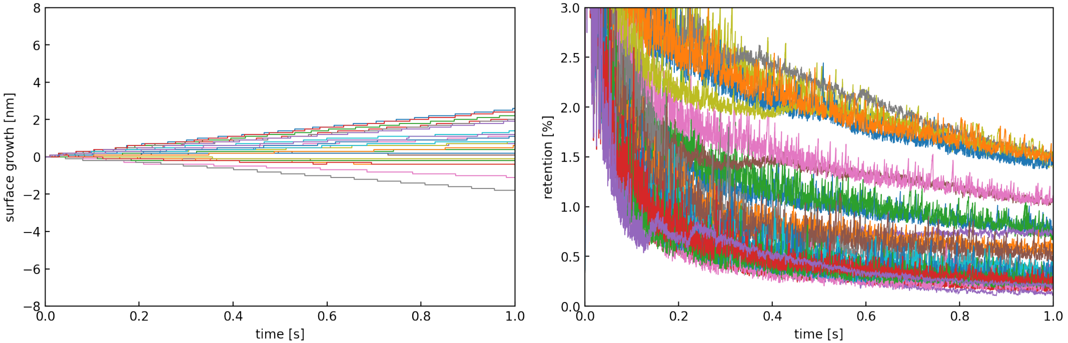

Coupled Xolotl-FTridyn (2/2)

- Output quantities of interest are surface growth and He retention as a function of time
- Illustration of 25 randomly chosen output samples
- Apply moving-average filter to output signal with δt = 0.1s to average over bubble bursts

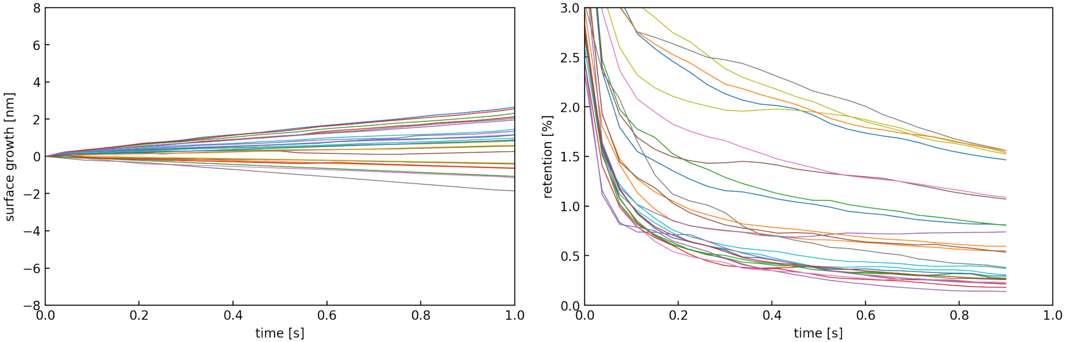

PCE surrogate construction for coupled F-Tridyn–Xolotl

- Construct surrogate models for predictions of surface growth (left) and He retention (right)
- PCE coefficients obtained using iterative BCS with 799 training samples and 100 validation samples, ~96 hours per sample on 2 nodes (136 cores) on Cori
- Agreement between model output and PCE prediction

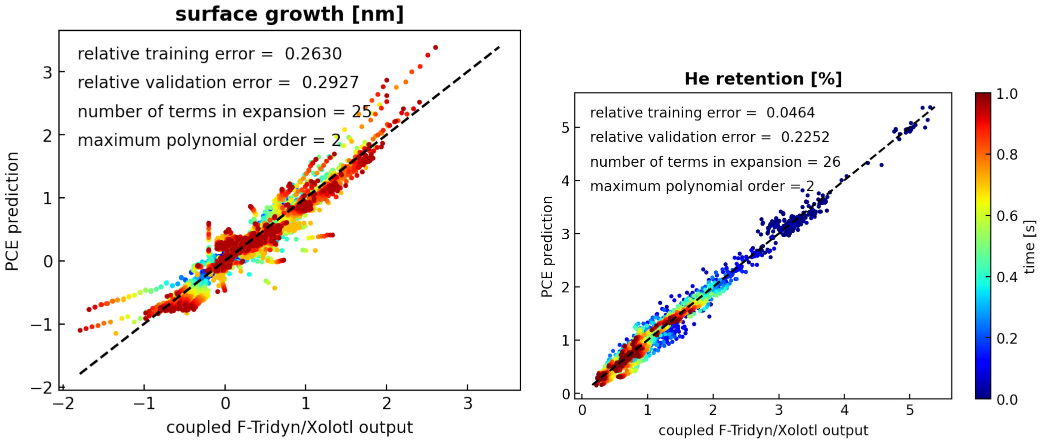

Global sensitivity analysis of coupled F-Tridyn–Xolotl (1/2)

- Evolution of the sensitivity indices for surface growth (left) and He retention (right) as a function of time
- 3 parameters (beam energy, tungsten surface binding energy and migration parameter He_1) are sufficient to explain $>$ 99% of the variability in the output

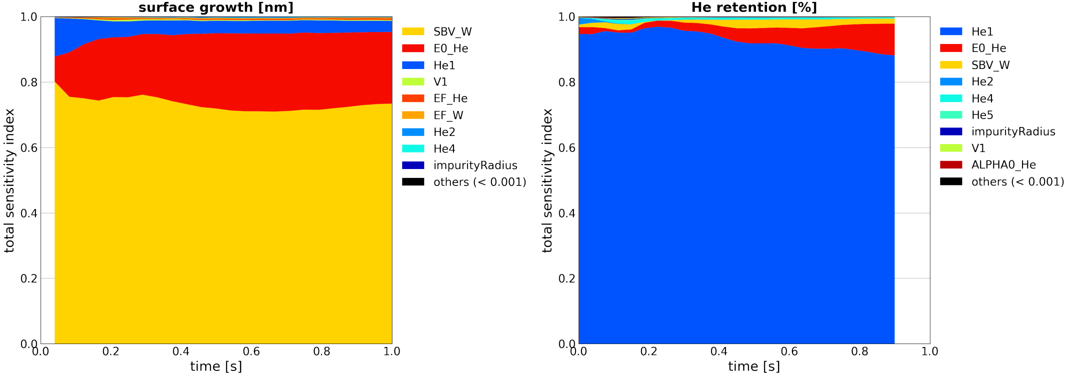

Global sensitivity analysis of coupled F-Tridyn–Xolotl (2/2)

- Convergence of the sensitivity indices for surface growth and He retention
- Values of the sensitivity indices stabilize after ~500 samples

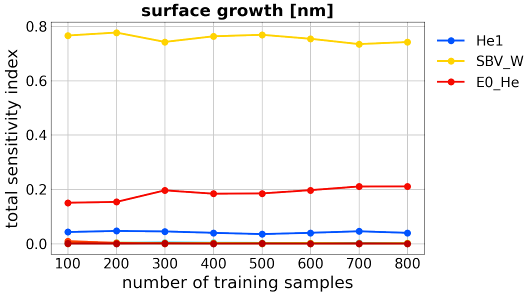

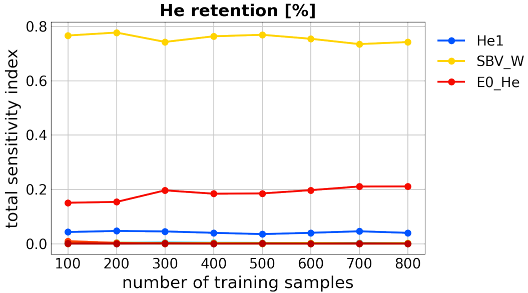

Multifidelity global sensitivity analysis of of coupled F-Tridyn–Xolotl

- Samples of the high-fidelity model $P^{\mathrm{high}}(\boldsymbol{x})$ use He cluster network size of 250
- Consider a low-fidelty model that uses a smaller network size (less He clusters to be tracked)
- Correlogram between high-fidelity and low-fidelity model output shows reasonable correlation for surface growth

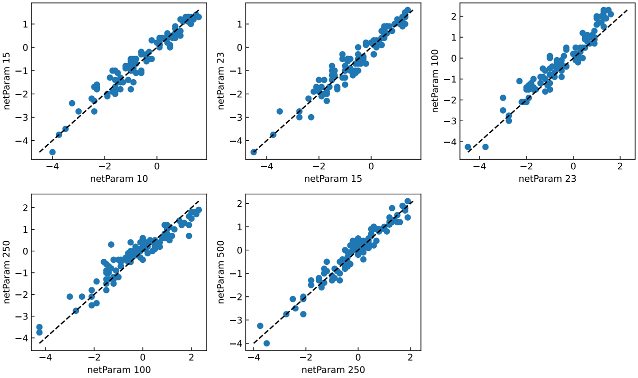

Multifidelity global sensitivity analysis of of coupled F-Tridyn–Xolotl

- Samples of the high-fidelity model $P^{\text{high}}(\boldsymbol{x})$ use He cluster network size of 250
- Consider a low-fidelty model that uses a smaller network size (less He clusters to be tracked)
- Correlogram between high-fidelity and low-fidelity model output shows poor correlation for surface growth

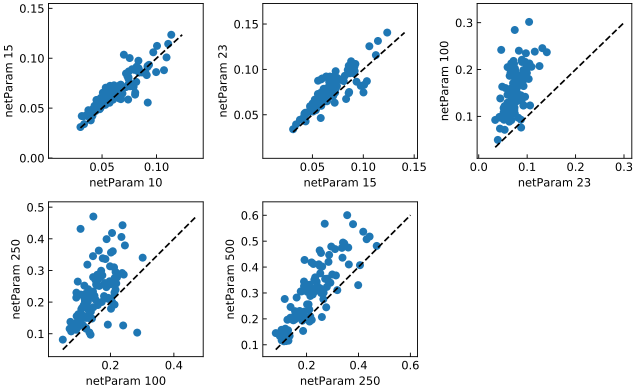

Conclusion and future work

- We performed global sensitivity analysis (GSA) of a coupled code used to predict the material evolution in plasma-surface interactions
- Our GSA approach uses polynomial chaos expansion (PCE) surrogate models
- We investigated the use of multifidelity PCE methods to alleviate the computational cost, with mixed success
  - Multifidelity PCE construction yields computational savings for GSA of `F-Tridyn` code in isolation
  - Only single-level GSA results available for the coupled setting (bubble bursting events?)
- Future research will focus on different experimental settings (ITER-He) and the use of other potential fidelity parameters (e.g., grid spacing)

Conclusion and future work

- We performed global sensitivity analysis (GSA) of a coupled code used to predict the material evolution in plasma-surface interactions
- Our GSA approach uses polynomial chaos expansion (PCE) surrogate models
- We investigated the use of multifidelity PCE methods to alleviate the computational cost, with mixed success
  - Multifidelity PCE construction yields computational savings for GSA of `F-Tridyn` code in isolation
  - Only single-level GSA results available for the coupled setting (bubble bursting events?)
- Future research will focus on different experimental settings (ITER-He) and the use of other potential fidelity parameters (e.g., grid spacing)

Thank you

References

- Adams, B., Bohnhoff, W., Dalbey, K., Ebeida, M., Eddy, J., Eldred, M., Hooper, R., Hough, P., Hu, K., Jakeman, J., et al. (2021). Dakota, a multilevel parallel object-oriented framework for design optimization, parameter estimation, uncertainty quantification, and sensitivity analysis: Version 6.15 user's manual. Technical report, Sandia National Lab.(SNL-NM), Albuquerque, NM (United States).
- Balay, S., Abhyankar, S., Adams, M. F., Benson, S., Brown, J., Brune, P., Buschelman, K., Constantinescu, E. M., Dalcin, L., Dener, A., Eijkhout, V., Gropp, W. D., Hapla, V., Isaac, T., Jolivet, P., Karpeev, D., Kaushik, D., Knepley, M. G., Kong, F., Kruger, S., May, D. A., McInnes, L. C., Mills, R. T., Mitchell, L., Munson, T., Roman, J. E., Rupp, K., Sanan, P., Sarich, J., Smith, B. F., Zampini, S., Zhang, H., Zhang, H., and Zhang, J. (2022). PETSc Web page. `https://petsc.org/`.
- Blondel, S., Bernholdt, D. E., Hammond, K. D., Hu, L., Maroudas, D., and Wirth, B. D. (2017). Benchmarks and tests of a multidimensional cluster dynamics model of helium implantation in tungsten. *Fusion Science and Technology*, 71(1):84–92.
- Crestaux, T., Le Maıtre, O., and Martinez, J.-M. (2009). Polynomial chaos expansion for sensitivity analysis. *Reliability Engineering & System Safety*, 94(7):1161–1172.
- Drobny, J., Hayes, A., Curreli, D., and Ruzic, D. N. (2017). F-TRIDYN: A Binary Collision Approximation code for simulating ion interactions with rough surfaces. *Journal of Nuclear Materials*, 494:278–283.

References (cont.)

- Elwasif, W. R., Bernholdt, D. E., Shet, A. G., Foley, S. S., Bramley, R., Batchelor, D. B., and Berry, L. A. (2010). The design and implementation of the swim integrated plasma simulator. In *18th Euromicro Conference on Parallel, Distributed and Network-based Processing*, pages 419–427.
- Ghanem, R. G. and Spanos, P. D. (2003). *Stochastic finite elements: a spectral approach*. Courier Corporation.
- Ng, L. W.-T. and Eldred, M. (2012). Multifidelity uncertainty quantification using non-intrusive polynomial chaos and stochastic collocation. In *53rd AIAA/ASME/ASCE/AHS/ASC Structures, Structural Dynamics and Materials Conference 20th AIAA/ASME/AHS Adaptive Structures Conference 14th AIAA*, page 1852.
- Sargsyan, K., Safta, C., Najm, H. N., Debusschere, B. J., Ricciuto, D., and Thornton, P. (2014). Dimensionality reduction for complex models via Bayesian compressive sensing. *International Journal for Uncertainty Quantification*, 4(1).
- Sobol, I. M. (2001). Global sensitivity indices for nonlinear mathematical models and their Monte Carlo estimates. *Mathematics and computers in simulation*, 55(1-3):271–280.
- Sudret, B. (2008). Global sensitivity analysis using polynomial chaos expansions. *Reliability engineering & system safety*, 93(7):964–979.

References (cont.)

- Wirth, B. et al. (2022). PSI2 Project Web page. `https://confluence.cels.anl.gov/display/PSIscidac2/Plasma+Surface+Interactions+2/`.
- Xiu, D. and Karniadakis, G. E. (2002). The Wiener–Askey polynomial chaos for stochastic differential equations. *SIAM journal on scientific computing*, 24(2):619–644.